Theory for Formation of a Low-Pressure, Current-Free Double Layer

M. A. Lieberman* and C. Charles

Space Plasma, Power and Propulsion, Research School of Physical Sciences and Engineering, Australian National University, ACT 0200, Australia

(Received 14 March 2006; published 26 July 2006)

A diffusion-controlled theory is developed for the formation of a low-pressure, current-free double layer just inside an upstream insulating source chamber connected to a larger diameter, downstream chamber. The double layer is described using four groups of charged particles: thermal ions, monoenergetic accelerated ions flowing downstream, accelerated electrons flowing upstream, and thermal electrons. The condition of particle balance upstream is found to determine the double layer potential. The double layer disappears at very low pressures due to loss of ionization balance upstream and due to energy relaxation processes for ionizing electrons at higher pressures, in good agreement with experiments.

DOI: 10.1103/PhysRevLett.97.045003 PACS numbers: 52.27.−h

Although double layers have been studied for decades, most theoretical papers have dealt with current-driven double layers [1]. There has been considerable interest in the formation of current-free double layers in low-pressure rf-driven plasmas [2–4] and in their application to such diverse fields as plasma thrusters for space propulsion [2,5] and the physics of the solar corona [5,6].

In one recent experiment [2,7], a plasma created by 13.56 MHz excitation of a helicon-type antenna wrapped around a cylindrical insulating source chamber (referred to as upstream region 2 of length $h = 31$ cm and radius $R_2 = 6.85$ cm) is connected to a larger diameter metallic expansion chamber (downstream region 1 of length $w = 29.4$ cm and radius $R_1 = 15.9$ cm). At argon pressures in the range 0.2–2 mTorr, ion energy analyzer measurements show that a thin double layer is formed in the source chamber a short distance from its junction with the expansion chamber. In this Letter, we develop a theory that couples the dynamics of the particles in the non-neutral double layer to the diffusive flows of the quasineutral plasmas in the source and expansion chambers.

Andrews and Allen [8] obtained conditions to embed a double layer in a quasineutral plasma using four groups of charged particles inside the double layer of potential V_s: (a) thermal ions, (b) accelerated ions flowing downstream, (c) accelerated electrons flowing upstream, and (d) thermal electrons. We follow the procedure of Ref. [8] but introduce an accelerated half-Maxwellian (f_{c1}), rather than a monoenergetic electron group, to more realistically describe the experiments [2,7]. The downstream distribution that is subsequently accelerated across the double layer is

$$f_{c1} = \begin{cases} \frac{2n_{c1}}{\mathrm{erfc}(\zeta_1)}\left(\frac{m}{2\pi e T_e}\right)^{1/2} e^{-mv_z^2/2eT_e} & v_z > v_e, \\ 0 & v_z > v_e, \end{cases} \qquad (1)$$

where $\zeta_1 = (mv_e^2/2eT_e)^{1/2}$, $n_{c1} = -\rho_{c1}/e$, erfc is the complementary error function, the normalization is $\int f_{c1} dv_z = n_{c1}$, and m, e, and T_e are the electron mass, charge, and temperature in equivalent voltage units, respectively. The velocity v_e is found to be of the order $(eT_i/m)^{1/2}$, which is much smaller than the electron thermal velocity for $T_i \ll T_e$, where T_i is the ion temperature.

At the low pressures of the experiments, the energy relaxation length for electrons with energies below the first excitation potential of argon ($\sim$11.6 V) is much larger than the system length. Therefore, we choose the same characteristic T_e for the accelerated group (c) as for the trapped electron group (d). Following the solution procedure detailed in Ref. [8], the density ratios of the four particle groups can be initially found at the downstream and upstream edges of the double layer for a given T_i/T_e and V_s/T_e, and the main results are shown in Fig. 1. The ratio of total downstream-to-upstream density n_1/n_2 as a function of the double layer strength V_s/T_e, for an assumed ion-to-electron temperature ratio $T_i/T_e = 0.05$, is nearly unity over the entire range of strengths (dotted line), and the accelerating ion group enters the double layer at a velocity of 1.2–1.3u_B (u_B is the Bohm velocity). The accelerated

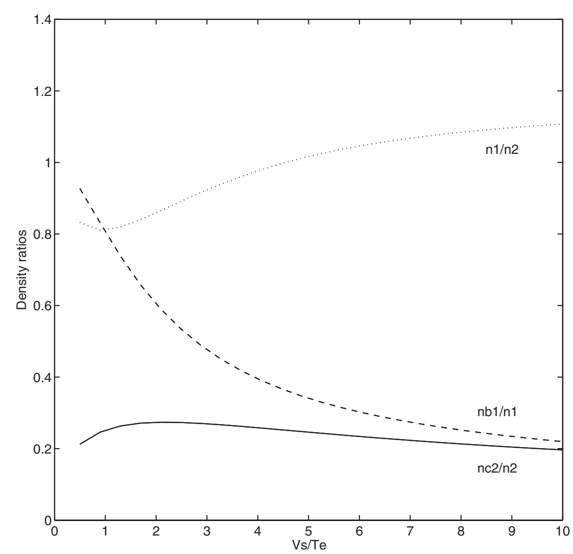

FIG. 1. n_1/n_2 (dotted line), n_{c2}/n_2 (solid line), and n_{b1}/n_1 (dashed line) density ratios versus double layer strength V_s/T_e.

electrons (solid line) comprise about 20% of the upstream density (n_{c2}/n_2), relatively independent of the ratio V_s/T_e. The densities for the accelerated ion group (dashed line) as a fraction of the total downstream density (n_{b1}/n_1) fall from nearly 100% to 20% over the range of V_s/T_e shown. Experimental measurements [7,9] show a double layer thickness of a few tens of Debye lengths $\lambda_{\rm De}$ (much thinner than the curvature scale length of the experimental magnetic field), which is consistent with a thickness of $\sim 10\lambda_{\rm De}\sqrt{V_s/T_e}$ given by Andrews and Allen (see Fig. 6 in Ref. [8] and the associated discussion).

The entire source chamber is insulating in the experiments, such that the net (electrical) current flowing into the source must vanish. A fifth species is introduced, which is formed by reflection of (almost) all of the accelerated electron group by the sheath at the upstream wall. The double layer solution is unaltered, and there is no fundamental distinction between a current-carrying and a current-free double layer [10]. A slight imbalance in currents between the incident and reflected accelerated and thermal electron groups balances the flow of ions to the upstream wall, with a resulting floating potential that forms across the sheath at the upstream wall [7]. The typical measured double layer potentials are not that large, and the density is relatively low in our system so that the power fluxes onto the walls remain low.

To obtain the electron temperature T_e at a given pressure p (and neutral gas density n_g), the downstream particle balance is determined by the low-pressure diffusion theory for an unmagnetized plasma (see [11], Sec. 10.2; see also Sec. 5.4 for magnetic effects) with the assumption that the thermal ion diffusion flux flowing upstream into the source chamber is negligible. The upstream particle balance is then subsequently used to determine V_s. Because the upstream radius is smaller than the downstream radius, an additional source of upstream ionization is required at low pressures, which is supplied by the accelerated group of electrons. We use a simplified one-dimensional diffusion model for the particle balance upstream. Letting n_i, $n_{d2} = n_i - n_{c2}$, and n_{c2} be the densities of ions, thermal electrons, and accelerated electrons, respectively, with the latter species assumed to be uniform in z, then the upstream diffusion equation is

$$-D_{A2}\frac{d^2 n_i}{dz^2} + \nu_R n_i = n_g(K_{iz}n_{d2} + K_{izc}n_{c2}), \qquad (2)$$

where $D_{A2} = h_{R_2}u_B R_2$ is a low-pressure ambipolar diffusion coefficient, n_g is the neutral gas density, $\nu_R = 2h_{R_2}u_B/R_2$ is the radial loss frequency, $h_{R_2} = 0.8/(4 + R_2/\lambda_i)^{1/2}$ is the edge-to-center radial density ratio (see [10], p. 148), λ_i is the thermal ion mean free path in argon, $K_{iz}(T_e)$ is the ionization rate coefficient for thermal (Maxwellian) electrons, and K_{izc} is the ionization rate coefficient for the accelerated electron group, which is a function of V_s and T_e. K_{izc} is calculated using the accelerated electron velocity distribution function f_{c2} by integration of $\sigma_{iz}vf_{c2}$ over velocity space, where σ_{iz} is the ionization cross section and v is the electron speed.

We use a symmetric solution for the ion density about $z = h/2$

$$n_i = \beta n_{c2} - n_{i0}\cosh\gamma(z - \tfrac{1}{2}h), \qquad (3)$$

where

$$\beta = \frac{n_g(K_{izc} - K_{iz})}{\nu_R - K_{iz}n_g}, \qquad (4)$$

and $\gamma^2 = (\nu_R - K_{iz}n_g)/D_{A2}$ is the square of the axial decay constant. Setting the ion flux $\Gamma_i = -D_{A2}(dn/dz) = n_i v_i$ at $z = h$ determines n_{i0}, where v_i is the velocity of the monoenergetic ions entering the double layer upstream. The complete solution is then

$$n_i = \left[1 - \frac{\cosh\gamma(z - \frac{1}{2}h)}{\frac{\gamma D_{A2}}{v_i}\sinh\frac{1}{2}\gamma h + \cosh\frac{1}{2}\gamma h}\right]\beta n_{c2}. \qquad (5)$$

Evaluating this equation at the upstream edge of the double layer $z = h$ yields

$$\beta = \left(1 + \frac{v_i}{\gamma D_{A2}}\coth\frac{1}{2}\gamma h\right)\frac{n_{i2}}{n_{c2}}, \qquad (6)$$

where $n_{i2} = n_{a2} + n_{b2}$ is the total ion density at the upstream edge. The ratio n_{i2}/n_{c2} is determined using the procedure in Ref. [8]. Equating (4) and (6) yields

$$\frac{n_g(K_{izc} - K_{iz})}{\nu_R - K_{iz}n_g} = \left(1 + \frac{v_i}{\gamma D_{A2}}\coth\frac{1}{2}\gamma h\right)\frac{n_{i2}}{n_{c2}}. \qquad (7)$$

Since K_{izc} and n_{i2}/n_{c2} depend on V_s, solving (7) numerically determines the double layer strength V_s needed for particle balance upstream.

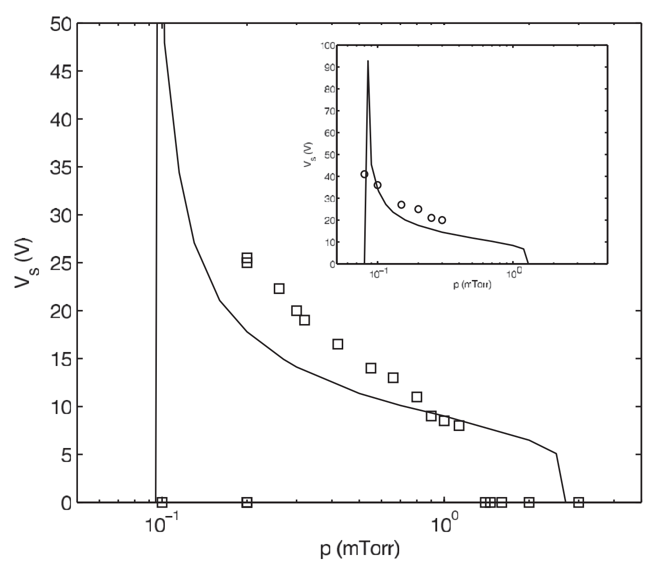

FIG. 2. Pressure variation of the double layer strength V_s: theoretical (solid line) and experimental (open squares) results; inset is for a larger device: measurements (open circles) from Ref. [9] and theory (solid line).

The results for V_s versus pressure p are given as the solid line in Fig. 2 and compared to the experiment (open squares). We see that V_s rises dramatically as the pressure is decreased, with a minimum pressure of approximately 0.1 mTorr for a solution to exist. Below that pressure, the maximum (with respect to V_s) ionization rate coefficient K_{izc} of $\sim 2.2 \times 10^{-13}$ $\mathrm{m^3/s}$ for the accelerated electrons upstream is not sufficient to balance the excess upstream particle losses. The maximum double layer strength can be as high as $\sim$100 V near the minimum pressure but is a very sensitive function of pressure for such high values of V_s. Both the experiment and theory show that the double layer disappears at pressures below 0.2 mTorr, although the plasma is maintained. The transition is marked by a strong decrease in density (factor of at least 4), so that the upstream density becomes much lower than the downstream density.

In the experiment, the double layer also disappears at pressures above about 1.5 mTorr. For a 20 V electron, the energy relaxation length for ionizing electrons (see [11], p. 691) is $\lambda_{iz} \approx 30$ cm at 1 mTorr, which is comparable to the system length. Since electrons are heated upstream, the downstream ionizing electron density can be depleted at the higher pressures. When the ratio of downstream-to-upstream ionization rates becomes equal to the ratio of downstream-to-upstream particle loss rates, then the additional ionization provided by electrons accelerated upstream by the double layer is no longer needed. An analytical estimate (see Fig. 2) shows that the double layer disappears at pressures above about 2.5 mTorr as is seen experimentally.

Downstream, the accelerated ions enter the expansion chamber, where they undergo charge transfer collisions with the neutral gas, leading to the production of thermal ions [7]. The neutralizing electrons associated with the downstream beam ions also lead to additional ionization. A simplified diffusion model is used, and the downstream beam ion density is

$$n_b = n_{b1} e^{-(z-h)/\lambda_b}, \tag{8}$$

where $\lambda_b \approx 0.7\lambda_i$ is the beam ion–neutral charge transfer mean free path. The net number of beam ions per second converted to thermal ions in the expansion chamber is $n_{b1} v_b (1 - e^{-w/\lambda_b}) \pi R_2^2$, where $v_b = (v_i + 2eV_s/M)^{1/2}$ is the beam ion velocity in the expansion chamber (M is the ion mass). Dividing by the volume of the expansion chamber, the volume rate of production of thermal ions is then $\nu_b n_{\mathrm{beff}}$, where $\nu_b = v_b/\lambda_b$ is the charge transfer frequency and

$$n_{\mathrm{beff}} = n_{b1} \frac{\lambda_b}{w} \frac{R_2^2}{R_1^2} (1 - e^{-w/\lambda_b}). \tag{9}$$

The diffusion equation for thermal ions downstream is

$$-D_{A1} \frac{d^2 n_i}{dz^2} + \nu_{R_1} n_i = n_g K_{iz} (n_i + n_{\mathrm{beff}}) + \nu_b n_{\mathrm{beff}}, \tag{10}$$

where $D_{A1} = h_{R_1} u_B R_1$ and h_{R_1} is expressed as h_{R_2}. The solution is

$$n_i = n_{a1} \cos k_1 (z - h) + \alpha n_{\mathrm{beff}} [\cos k_1 (z - h) - 1], \tag{11}$$

where $k_1^2 = (n_g K_{iz} - \nu_{R_1})/D_{A1}$ is the square of the downstream axial wave number, and

$$\alpha = \frac{k_1^2 D_{A1} + \nu_{R_1} + \nu_b}{k_1^2 D_{A1}}. \tag{12}$$

Setting the thermal ion flux $\Gamma_i = n_i u_B$ at $z = h + w$ yields

$$k_1 D_{A1} (n_{a1} + \alpha n_{\mathrm{beff}}) \sin k_1 w = u_B (n_{a1} + \alpha n_{\mathrm{beff}}) \cos k_1 w - u_B \alpha n_{\mathrm{beff}}. \tag{13}$$

Solving (13) for k_1, we obtain the density profile from (11); k_1 is found to be real at low pressures and imaginary at higher pressures.

The potential distribution in the discharge is determined from the density distribution. With the zero of potential at the downstream wall and a floating potential of $V_{f1} = \frac{1}{2} T_e \ln(2M/\pi m) = 5.4 T_e$ across the sheath there [12], the

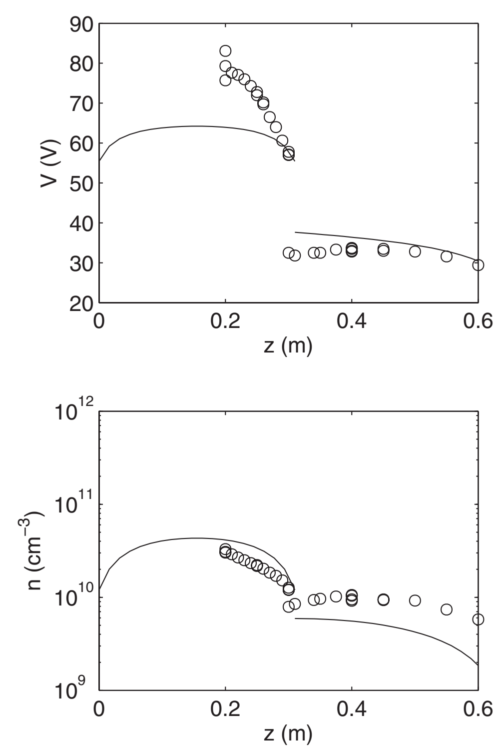

FIG. 3. Theoretical (solid line) and experimental (open circles from Ref. [2]) results of potential (top) and thermal ion density (bottom) versus position z at 0.2 mTorr; to facilitate the visual comparison with the theory, the double layer measured at $z = 0.25$ m is positioned at $z = 0.30$ m, i.e., at the junction between regions 1 and 2.

downstream potential is

$$V_1(z) = 5.4T_e + T_e \ln(n_e(z)/n_e(h + w)). \quad (14)$$

The upstream potential is

$$V_2(z) = V_1(h) + V_s + T_e \ln(n_{d2}(z)/n_{d2}(h)). \quad (15)$$

The floating potential V_{f2} at the upstream wall is obtained by equating the ion and electron fluxes there. Figure 3 shows the theoretical results (solid lines) for the potential and the thermal ion density at 0.2 mTorr, for comparison to the experimental results (open circles) published in Ref. [2]. The calculated potential (with respect to Earth) at the upstream wall is about 12 V at 0.2 mTorr. The general shape of the potential and the thermal ion density is quite similar to that seen experimentally, but with a somewhat smaller double layer potential V_s. However, V_s is a quite sensitive function of pressure in this range, and a small decrease in the pressure will give a better match to the experimental result for V_s. An unexplained feature of the experimental results, not seen in the theory, is the large potential rise upstream of the double layer, which may be an artifact of the experimental measurement for z less than 0.2 m, where a non-negligible earthed area (probe shaft) is introduced into the insulated region 2 [7]. At 0.2 mTorr, the calculated T_e and V_s are 5.8 and 17.8 V, respectively, which gives a V_s/T_e ratio of 3, similar to that found experimentally [2]. Figure 3 shows that the calculated and measured thermal ion density drops by a factor of about 2 at the double layer position. However, the total density ratio n_1/n_2 remains close to unity for all values of V_s/T_e (Fig. 1), a feature not yet measured in our device.

In another experiment in a larger device ($h = 57.8$ cm, $R_2 = 10$ cm, $w = 200$ cm, $R_1 = 50$ cm), the double layer potential was measured by Sutherland *et al.* [9] over a somewhat limited range of pressures in argon. The experimental results (open circles in the inset in Fig. 2) are in good agreement with the theoretical curve (solid line).

Previous experimental and simulation studies [2–4,13] agreed on the formation of an energetic ion beam with a correlation between the potential drop of the double layer and the accelerated ion velocity. In the simulation results by Meige *et al.* [13], the density depends on the plasma potential through the classical Boltzmann equation which gives a typical density decrease of a factor of 10 between the upstream and downstream sides of the double layer, while the measured decrease is a factor of 1 to 3. This Letter provides a new understanding of the density which agrees with the experiment. It shows that the population of accelerated electrons in the helicon source comprises about 20% of the upstream density, which is in good agreement with a minimum estimated value of 12% obtained by Charles and Boswell from Langmuir probe data [7]. However, other experiments on different devices indicate either a possible weak beam [14] or no beam at all [15].

In the context of plasma propulsion, a different theoretical model of current-free double layers has been developed by Fruchtman [5]. While in Ref. [5] thrust is imparted to the plasma at the double layer itself by the magnetic field pressure, in the present model, no thrust is imparted to the plasma at the double layer but only at the back wall, where the electrons accelerated backwards by the double layer are reflected [16].

The velocity of the ions entering the double layer at the upstream side has been found to be about u_B in laser induced fluorescence experiments and in the simulation [4] but up to twice u_B in energy analyzer experiments [7]. In the present theory, a value of 1.2–1.3 times u_B is found, similar to that derived in Ref. [8], which is within the experimental range. Ions enter the sheath at the axial end of the expansion region with u_B due to sufficient ion-neutral collisions.

Although the present theory does not address double layers in electronegative discharges [17], future work will be carried out for other gases, and our model, presently validated for two different size devices exhibiting double layer formation, may be applicable to other helicon double layer experiments such as that of Cohen *et al.* [3], who measured typical axial ion energies of 17 eV for a pressure of 0.15 mTorr in the expansion region.

*Permanent address: Department of Electrical Engineering and Computer Science-1770, University of California, Berkeley, CA 94720, USA.

[1] M. A. Raadu, Phys. Rep. **178**, 25 (1989).
[2] C. Charles and R. W. Boswell, Appl. Phys. Lett. **82**, 1356 (2003).
[3] S. A. Cohen *et al.*, Phys. Plasmas **10**, 2593 (2003).
[4] X. Sun *et al.*, Phys. Rev. Lett. **95**, 025004 (2005).
[5] A. Fruchtman, Phys. Rev. Lett. **96**, 065002 (2006).
[6] R. W. Boswell, E. Marsch, and C. Charles, Astrophys. J. **640**, L199 (2006).
[7] C. Charles and R. W. Boswell, Phys. Plasmas **11**, 3808 (2004).
[8] J. G. Andrews and J. E. Allen, Proc. R. Soc. A **320**, 459 (1971).
[9] O. Sutherland *et al.*, Phys. Rev. Lett. **95**, 205002 (2005).
[10] C. Chan, N. Hershkowitz, and G. L. Payne, Phys. Lett. **83A**, 328 (1981).
[11] M. A. Lieberman and A. J. Lichtenberg, *Principles of Plasma Discharges and Materials Processing* (Wiley, New York 2005), 2nd ed., Sec. 10.2, pp. 148 and 691 and Sec. 5.4, pp. 140–145.
[12] F. Chen, Phys. Plasmas **8**, 3029 (2001).
[13] A. Meige *et al.*, Phys. Plasmas **12**, 052317 (2005).
[14] R. T. S. Chen and N. Hershkowitz, Phys. Rev. Lett. **80**, 4677 (1998).
[15] F. F. Chen and D. D. Blackwell, Phys. Rev. Lett. **82**, 2677 (1999).
[16] F. N. Gesto *et al.*, J. Propul. Power **22**, 24 (2006).
[17] N. Plihon, C. S. Corr, and P. Chabert, Appl. Phys. Lett. **86**, 091501 (2005).